Int. J. Heat Mass Transfer. Vol. 26, No. 9, pp. 1339–1346, 1983
Printed in Great Britain

0017-9310/83 $3.00 + 0.00

THE BOUNDARY LAYER REGIME IN A POROUS LAYER WITH UNIFORM HEAT FLUX FROM THE SIDE†

ADRIAN BEJAN
Department of Mechanical Engineering, Campus Box 427, University of Colorado, Boulder, CO 80309, U.S.A.

(*Received* 16 *August* 1982 *and in revised form* 17 *December* 1982)

Abstract—This paper reports an analytical solution and a numerical study of natural convection in a rectangular porous layer heated and cooled with uniform heat flux along the vertical side walls. It is shown analytically that in the boundary layer regime the vertical boundary layer thickness is constant (independent of altitude) and the core region is motionless. The vertical temperature gradient is the same constant everywhere in the porous layer. Numerical results are reported in the range $100 < Ra < 5000$, $1 \leqslant H/L \leqslant 10$, where $Ra = Kg\beta H^2 q''/(\alpha\nu k)$. The boundary layer analytical solution is shown to agree well with the numerical results.

NOMENCLATURE

- c_p specific heat at constant pressure
- g gravitational acceleration
- H vertical dimension
- k thermal conductivity of fluid-saturated porous medium
- K permeability
- L horizontal dimension
- q'' constant heat flux
- Ra Darcy–Rayleigh number, equation (10)
- T temperature
- T_∞ core temperature
- ΔT wall-to-wall temperature difference at y = constant
- u horizontal velocity component
- u_∞ horizontal velocity in the core region
- v vertical velocity component
- x horizontal position
- y vertical position
- z horizontal position measured with respect to the right wall (Fig. 1)

Greek symbols

- α thermal diffusivity, $k/(\rho c_p)_{fluid}$
- β coefficient of thermal expansion
- δ boundary layer thickness
- λ Oseen function
- ν kinematic viscosity
- ρ density
- ψ streamfunction
- ψ_∞ core streamfunction

Subscripts

- $()_*$ dimensionless variables, equations (14)
- $()_R$ solution near the right wall (Fig. 1)

1. INTRODUCTION

THE HEAT transfer by natural convection across a porous medium heated from the side is a topic of fundamental importance in diverse fields such as thermal insulation engineering, geothermal reservoir dynamics and grain storage. The basic model used so far in the study of porous media heated from the side consists of a 2-dim. layer with vertical isothermal walls at different temperatures and with adiabatic top and bottom walls. This model has been investigated extensively during the past 20 years, experimentally [1–3] and numerically [4–7]. On the theoretical front, Weber [8] reports an Oseen-linearized analysis of the boundary layer regime in a tall layer: Weber's analysis was improved by the present author [9] to account for the heat transfer vertically through the core and, in this way, to predict correctly the heat transfer rates revealed by experiments and by numerical simulations. An integral-type analysis of the same boundary layer regime was reported by Simpkins and Blythe [10] and, for temperature-dependent viscosity, by Blythe and Simpkins [11]. The corresponding flow in a shallow layer heated from the side was documented by Walker and Homsy [12] and Bejan and Tien [13].

The object of the present study is to discuss an equally plausible situation for the natural convection phenomenon, namely, heat transfer through the same 2-dim. porous layer when, instead of temperatures, uniform heating and cooling effects are prescribed along the vertical side walls. This model has not been studied before. At least from the point of view of thermal insulation engineering, this new model is more appropriate, particularly if we recognize that isothermal side walls are never a feature of fibrous and granular vertical insulating layers in the building technology. Vertical solid surfaces separating fluids which exchange heat by natural convection always 'float' naturally to a state closely resembling the 'uniform heat flux' condition [14]. The engineering importance of the uniform heat flux wall model was recognized early in the study of natural convection along a single wall facing a fluid [15] and along a single wall facing a fluid-saturated porous medium [16].

2. BOUNDARY LAYER SCALING

Consider the 2-dim. rectangular porous layer shown in Fig. 1. The system is heated along the right side and

† Dedicated to the memory of Werner Schultz (1955–1982) of the University of Stuttgart.

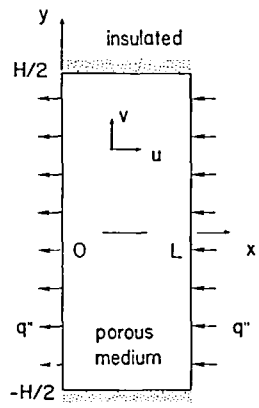

FIG. 1. Schematic of 2-dim porous layer with uniform heat flux from the side.

cooled along the left side uniformly, i.e.

$$q'' = k\left(\frac{\partial T}{\partial x}\right)_{x=0,L} = \text{constant}. \tag{1}$$

The top and bottom surfaces of the porous medium are insulated. The equations governing the conservation of mass, momentum and energy at any point (x, y) are [8]

$$\frac{\partial u}{\partial x} + \frac{\partial v}{\partial y} = 0, \tag{2}$$

$$\frac{\partial u}{\partial y} - \frac{\partial v}{\partial x} = -\frac{Kg\beta}{\nu}\frac{\partial T}{\partial x}, \tag{3}$$

$$u\frac{\partial T}{\partial x} + v\frac{\partial T}{\partial y} = \alpha\left(\frac{\partial^2 T}{\partial x^2} + \frac{\partial^2 T}{\partial y^2}\right). \tag{4}$$

These equations correspond to having modeled the porous medium as homogeneous, so that $u, v, T, K, g, \beta, \alpha$ represent the volume-averaged fluid velocity components, the local equilibrium temperature between fluid and porous solid, the permeability of the porous matrix, the gravitational acceleration, the coefficient of thermal expansion of the fluid, and the thermal diffusivity $k/(\rho c_p)_{\text{fluid}}$, respectively. The momentum equation (3) contains also the Boussinesq approximation whereby the fluid density ρ was taken as equal to $\rho_0[1-\beta(T-T_0)]$ only in the body force term. The derivation of equations (2)–(4) is outlined in greater detail in earlier papers on natural convection through porous media [4–8]: thus, the conductivity k is the stagnant thermal conductivity of the fluid-saturated porous medium, while the other properties belong to the flowing fluid.

Of special interest is the buoyancy-induced circulation in the boundary layer regime, where most of the fluid motion is restricted to a thin layer δ along each vertical wall. In order to determine analytically the flow and temperature field in each boundary layer region, it is absolutely essential that the scales governing each region are determined in advance. This problem is analogous to scaling analyses presented earlier for porous layers with isothermal side walls [8, 10]: what makes the present problem new is the uniform heat flux condition maintained on both vertical walls, equation (1). Recognizing δ and H as the x and y scales in the boundary layer region of interest ($\delta \ll H$), the conservation statements (2)–(4) require the following balances:

$$\frac{u}{\delta} \sim \frac{v}{H}, \tag{5}$$

$$\left(\frac{u}{H} \text{ or } \frac{v}{\delta}\right) \sim \frac{Kg\beta}{\nu}\frac{T}{\delta}, \tag{6}$$

$$\left(u\frac{T}{\delta} \text{ or } v\frac{T}{H}\right) \sim \alpha\left(\frac{T}{\delta^2} \text{ or } \frac{T}{H^2}\right). \tag{7}$$

In addition, the uniform heat flux condition (1) requires

$$q'' \sim k\frac{T}{\delta} = \text{constant}. \tag{8}$$

Noting that in the boundary layer region $(\delta/H) \ll 1$, the four statements (5)–(8) may be used to determine the four unknown scales,

$$\begin{aligned} \delta &\sim H\,Ra^{-1/3}, \\ T &\sim \frac{q''}{k}H\,Ra^{-1/3}, \\ v &\sim \frac{\alpha}{H}Ra^{2/3}, \\ u &\sim \frac{\alpha}{H}Ra^{1/3} \end{aligned} \tag{9}$$

where Ra is the Darcy–Rayleigh number based on heat flux and height,

$$Ra = \frac{Kg\beta H^2 q''}{\alpha\nu k}. \tag{10}$$

It is worth examining the present scaling results (9) and noting the differences between them and the corresponding results for porous layers with isothermal vertical walls [8, 10]. The fundamental difference is that in the present case the heat flux is fixed, while everything else, including the temperature scale, must adjust in accordance with the value of q'' (i.e. with the value of Ra).

The boundary layer scales (9) suggest the following nondimensionalization of the governing equations (2)–(4) in the boundary layer region

$$\frac{\partial u_*}{\partial x_*} + \frac{\partial v_*}{\partial y_*} = 0, \tag{11}$$

$$\frac{\partial v_*}{\partial x_*} = \frac{\partial T_*}{\partial x_*}, \tag{12}$$

$$u_*\frac{\partial T_*}{\partial x_*} + v_*\frac{\partial T_*}{\partial y_*} = \frac{\partial^2 T_*}{\partial x_*^2} \tag{13}$$

where

$$x_* = \frac{x}{H\,Ra^{-1/3}}, \quad y_* = \frac{y}{H},$$

$$u_* = \frac{u}{\frac{\alpha}{H}Ra^{1/3}}, \quad v_* = \frac{v}{\frac{\alpha}{H}Ra^{2/3}}, \tag{14}$$

$$T_* = \frac{T}{\frac{q''}{k}H\,Ra^{-1/3}}.$$

Using the same notation, the uniform heat flux condition (1) becomes

$$\frac{\partial T_*}{\partial x_*} = 1 \quad \text{at} \quad x_* = 0, \quad \text{and at} \quad x_* = \frac{L}{H}Ra^{1/3}. \tag{15}$$

As shown in the next section, the reward for having conducted the scaling analysis is that the dimensionless governing equations (11)–(13) have *exactly* the same form as for other boundary layer flows studied in the past. Thus, in order to solve equations (11)–(13) it is wise to rely on existing (proven) analytical methods such as the Oseen linearization technique used by Weber [8] in the case of porous layers with isothermal side walls.

3. ANALYTICAL SOLUTION

As discussed in Weber [8] as well as in a number of more recent analyses of natural convection in porous layers with isothermal walls [14, 17, 18], one way to solve the boundary layer equations (11)–(13) is by regarding u_* and $\partial T_*/\partial y_*$ as functions of y_* only, on the LHS of equation (13). The consequence of this linearization decision is an exponentially-varying velocity and temperature field in the vicinity of the vertical walls. Omitting the algebra described already in ref. [8], for the boundary layer lining the left (cold) wall in Fig. 1 we obtain

$$v_* = -\frac{1}{\lambda}e^{-\lambda x_*}, \tag{16}$$

$$T_* = -\frac{1}{\lambda}e^{-\lambda x_*} + T_{*\infty}(y_*). \tag{17}$$

The temperature profile (17) satisfies already the uniform heat flux condition at $x_* = 0$, equation (15). In general, the parameter λ is a function of y_*: this function is determined from energy integral condition [8]

$$\int_0^\infty \left(u_*\frac{\partial T_*}{\partial x_*} + v_*\frac{\partial T_*}{\partial y_*}\right)dx_* = \left|\frac{\partial T_*}{\partial x_*}\right|_0^\infty \tag{18}$$

which in the present case yields

$$\frac{d}{dy_*}\left(\frac{1}{2\lambda^3}\right) = \frac{T'_{*\infty}}{\lambda^2} - 1. \tag{19}$$

Function $T_{*\infty}(y_*)$ is unknown and represents the temperature distribution in the 'core', i.e. sufficiently far from the boundary layer region. In general, the core is also characterized by horizontal fluid motion (because $v_* \to 0$ as $x_* \to \infty$). The horizontal core velocity $u_{*\infty}$ follows from the continuity equation (11) combined with equation (16) in the limit $x_* \to \infty$,

$$u_{*\infty} = \frac{d}{dy_*}\left(\frac{1}{\lambda^2}\right). \tag{20}$$

According to the Oseen solution 'matching' approach described by Weber [8] and, earlier, by Gill [19], the unknowns $(\lambda, T_{*\infty}, u_{*\infty})$ are determined based on the energy integral (19) and the condition that the core flow must be centrosymmetric about $x = L/2$, $y = 0$ on Fig. 1. To the present solution, the centrosymmetry property means that

$$T_{*\infty} = \text{odd function of } y_*, \tag{21}$$

$$T'_{*\infty} = \text{even function of } y_*, \tag{22}$$

$$u_{*\infty} = \text{odd function of } y_*. \tag{23}$$

Equation (20) states that in order for $u_{*\infty}$ to be an odd function of y_*, the unknown function $1/\lambda^2$ must be even in y_*. But $1/\lambda$ represents the dimensionless boundary layer thickness (a positive finite quantity), hence, if $1/\lambda^2$ is an even function of y_* then $1/\lambda$ and λ are also symmetric about $y_* = 0$. In conclusion, the centrosymmetry property of the core also requires

$$\lambda = \text{even function of } y_*. \tag{24}$$

Finally, we examine the make-up of the energy integral condition (19) and recognize that: (1) the RHS is always an even function of y_* and (2) the LHS is always an odd function of y_*. This means that the only solution capable of satisfying equation (19) and the centrosymmetry conditions (21)–(24) is the one which makes both sides of equation (19) zero simultaneously. Therefore, the solution is

$$\lambda = \text{constant},$$

$$T_{*\infty} = \lambda^2 y_*, \tag{25}$$

$$u_{*\infty} = 0.$$

At this juncture, the important conclusion is that in the boundary layer regime of a porous layer with uniform heat flux the core is motionless ($v_{*\infty} = u_{*\infty} = 0$) and linearly stratified ($T'_{*\infty} = \lambda^2 = \text{constant}$). Furthermore, the boundary layer thickness $1/\lambda$ is constant, however, unknown at this point. Compared with the core and boundary layer flows developed by Weber for porous layers with isothermal walls, the present solution is strikingly simple. In fact, the simplicity of this solution led the present author to doubt it for about 6 months and, in the meantime, to conduct a complete numerical simulation of the phenomenon: the numerical results are reported in the next section, demonstrating that the analytical solution is indeed correct.

The solution is finally completed by determining the unknown constant λ: this constant must come from the

only geometric fact left out of the discussion so far, namely, the fact that the horizontal dimension of the system is L. [Note that so far L does not appear in the solution represented by equations (16), (17) and (25).] As we search for λ, we come across another interesting property of the flow pattern considered in this paper. As shown in Fig. 2, the two boundary layer streams move parallel to the vertical walls. Let $\dot{m}$ be the flowrate of each stream, and ΔT the 'average' temperature difference between streams at any $y = \text{constant}$. Consider now the control volume shown with a dashed line: the vertical stream counterflow pours energy into the control volume at a rate $\dot{m}c_p\Delta T$. Since the heat transfer collected by the control volume over the right wall leaves through the left wall unchanged, and since the top wall is insulated, the enthalpy inflow $\dot{m}c_p\Delta T$ must be balanced exactly by thermal diffusion across the arbitrary $y = \text{constant}$ surface. Thus at any level y along the boundary layer, the enthalpy convected upward by the boundary layer counterflow is always balanced by vertical heat conduction through the cross section L,

$$\int_0^L \rho c_p v T \, dx = \int_0^L k \frac{\partial T}{\partial y} dx, \quad \text{at any } y = \text{constant}. \tag{26}$$

It is worth noting that the control volume analysis of Fig. 2 was used previously in the context of natural convection in porous layers (e.g. ref. [9]). However, this is the first time that equation (26) applies exactly, because the heat flux is the same on both sides of the layer. The LHS of equation (26) is easily evaluated by breaking the integral into two parts, one for each boundary layer,

$$\int_0^L \rho c_p v T \, dx = \int_0^\infty \rho c_p v T \delta \, dx_* + \int_0^\infty \rho c_p v_R T_R \delta \, dz_*. \tag{27}$$

The new coordinate z is the horizontal position measured away from the heated wall ($z = L - x$, $z_* = z/\delta$). The dimensionless velocity and temperature profiles along the right wall (subscript R) are obtained by following the procedure leading to equations (16) and (17)

$$v_{R*} = \frac{1}{\lambda} e^{-\lambda z_*}, \tag{28}$$

$$T_{R*} = \frac{1}{\lambda} e^{-\lambda z_*} + T_{*\infty}. \tag{29}$$

Substituting expressions (16), (17) and (28), (29) into equation (27), the control volume energy conservation (26) yields the value of λ,

$$\lambda = \left(\frac{H}{L}\right)^{1/5} Ra^{1/15}. \tag{30}$$

At this point, the boundary layer solution is complete. In order to compare it most effectively with the numerical solution outlined in the next section, it is useful to calculate 'overall' theoretical quantities such as the mass flowrate of one boundary layer and the average temperature difference between the vertical walls. In dimensionless form, the boundary layer flowrate is the same as the 'core' value of the streamfunction ($u = \psi_y$, $v = -\psi_x$), in other words

$$\psi_{*\infty} = -\int_0^\infty v_* \, dx_* = \frac{1}{\lambda^2} = \left(\frac{H}{L}\right)^{-2/5} Ra^{-2/15}. \tag{31}$$

The temperature difference ΔT between the two walls is independent of y, because in the boundary layer regime the temperature of each vertical wall varies linearly in y, in precisely the same manner as the core temperature $T_{*\infty}(y_*)$. In dimensionless form, the overall temperature difference is

$$\Delta T_* = (T_{R*})_{z=0} - (T_*)_{x=0} = \frac{2}{\lambda} = 2\left(\frac{H}{L}\right)^{-1/5} Ra^{-1/15}. \tag{32}$$

Noting that $\Delta T_* = \Delta T/[(q''/k)H\, Ra^{-1/3}]$, equation (32) is equivalent to predicting the overall Nusselt number

$$Nu = \frac{(q''/\Delta T)H}{k} = \frac{Ra^{1/3}}{\Delta T_*} = \frac{1}{2}\left(\frac{H}{L}\right)^{1/5} Ra^{2/5}. \tag{33}$$

The purpose of the next section is to test numerically the analytical solution developed above for the boundary layer regime. Before performing this test, however, it is interesting to note that the Nusselt number predicted by equation (33) disagrees in a *scaling sense* with predictions available up to this point based on the isothermal-wall model. For example, translated into the notation of equation (33), Weber's Nusselt number [8] reads $Nu = 3^{-1/3} Ra^{1/3}$.

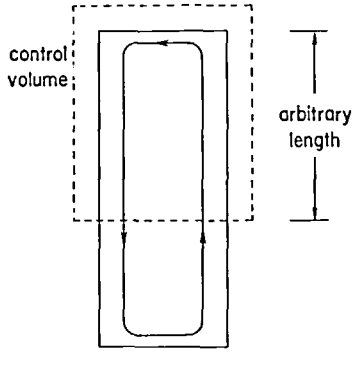

FIG. 2. Control volume argument showing that the net upflow of enthalpy must be balanced by conduction downward, at any level y.

4. NUMERICAL SOLUTION

A finite difference scheme was employed in order to solve the steady-state governing equations (2)–(4) for a given set of H/L and Ra. The complete equations (2)–(4) were first placed in dimensionless form by using the boundary layer scaling (9),

$$\frac{\partial^2 \psi_*}{\partial x_*^2} + Ra^{-2/3} \frac{\partial^2 \psi_*}{\partial y_*^2} = -\frac{\partial T_*}{\partial x_*}, \tag{13}$$

Table 1. Summary of numerical results for natural convection in a 2-dim. porous layer with uniform heat flux from the side

H/L	Ra	$\psi_{*\max}$	$\psi_{*\infty}$	$(\Delta T_*)_{y_*=0}$	$(\Delta T_*)_{y_*=\pm 1/2}$	$(\Delta T_*)_{eq.(32)}$	λ
1	100	0.470	0.541	1.808	2.392	1.471	1.359
	200	0.464	0.493	1.652	2.434	1.405	1.424
2	200	0.327	0.374	1.277	1.806	1.223	1.635
	400	0.329	0.341	1.216	1.859	1.168	1.713
	1000	0.312	0.302	1.154	1.891	1.099	1.821
4	500	0.207	0.251	†	1.386	1.002	1.997
	1000	0.222	0.229	1.028	1.437	0.956	2.091
	2000	0.228	0.208	†	1.454	0.913	2.190
	4000	0.223	0.190	†	1.448	0.872	2.294
10	5000	0.1272	0.1279	†	1.020	0.715	2.796

† Due to the limited output capability of the personal computer, these values were not recorded.

$$\frac{\partial\psi_*}{\partial y_*}\frac{\partial T_*}{\partial x_*}-\frac{\partial\Psi_*}{\partial x_*}\frac{\partial T_*}{\partial y_*}=\frac{\partial^2 T_*}{\partial x_*^2}+Ra^{-2/3}\frac{\partial^2 T_*}{\partial y_*^2}. \quad (14)$$

The boundary conditions corresponding to this formulation are

$$\psi_*=0,\quad \frac{\partial T_*}{\partial y_*}=0,\quad \text{at } y_*=\pm\frac{1}{2},$$

$$\psi_*=0,\quad \frac{\partial T_*}{\partial x_*}=1,\quad \text{at } x_*=0 \text{ and } x_*=\frac{L}{H}Ra^{1/3}. \quad (15)$$

Finite difference approximations of equations (13) and (14) were obtained by applying the scheme described in detail by Bankvall [5]. The $0<x_*<L/\delta$ interval was divided into N_x equal segments separated by N_x+1 nodes. Likewise, the $-\frac{1}{2}<y_*<\frac{1}{2}$ interval was divided into N_y segments. The numerical work started with postulating a certain distribution of flow and temperature, namely, no-flow ($\psi_*=0$ everywhere) and pure conduction ($T_*=x_*$). Based on these assumed fields, the momentum equation (13) was used to update, node-by-node, the ψ_* field. Next, the energy equation (14) was used in the same manner to update the T_* field. The values of T_* on the four boundaries were calculated from three-node approximations of the temperature gradient normal to the wall [equation (15)]. The numerical work of updating the ψ_* and T_* fields was repeated until the changes in ψ_* and T_* at any node became small enough to satisfy the convergence criterion

$$\left|\frac{(\psi_*,T_*)_{new}-(\psi_*,T_*)_{old}}{(\psi_*,T_*)_{old}}\right|\leqslant 10^{-6}. \quad (16)$$

Ten different cases ($H/L, Ra$) were solved numerically: Table 1 lists the main results of the numerical solution in each case. Except for the last case ($H/L=10$, $Ra=5000$), the present solutions were obtained using the grid $N_x=N_y=16$. This grid proved adequate in the sense that finer grids led to ΔT_* and $\psi_{*\infty}$ values within 1% of the values listed in Table 1. Convergence was achieved after 1000–1200 iterations; speed of execution was not a critical issue since the entire work was done on a personal computer (Apple II). The grid used for the last case of Table 1 was $N_x=16$, $N_y=20$, and convergence occurred after 2900 iterations. The acceptable performance of the personal computer *vis-à-vis* 'accuracy' in natural convection was documented by the present author in an earlier article [20].

Figures 3 and 4 show the temperature distribution along the two vertical walls and in the vertical midplane of the porous layer (at $x=L/2$). This figure is presented in order to test the chief property of the theoretical solution, namely, the linear variation of temperature with altitude, regardless of x. The numerical curves show clearly that almost throughout the cavity the temperature varies linearly with altitude. The thermal stratification is independent of x, hence, the wall-to-wall temperature difference is practically constant for most of the layer height H. Deviations from the theoretically predicted pattern occur near the top and bottom extremities where the vertical temperature

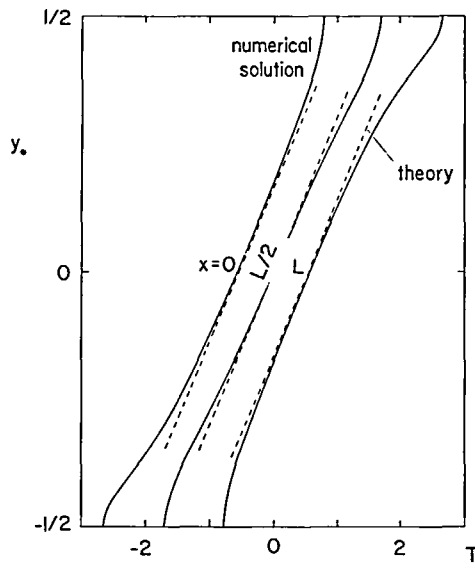

FIG. 3. Numerical vs theoretical temperature distribution in three vertical planes ($H/L=2$, $Ra=1000$).

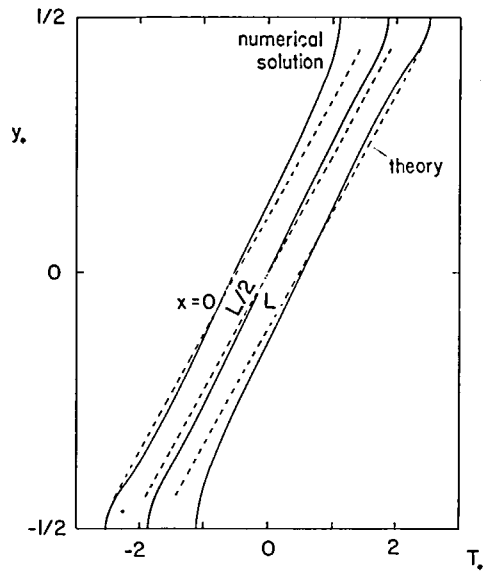

FIG. 4. Numerical vs theoretical temperature distribution in three vertical planes ($H/L = 4$, $Ra = 1000$).

gradient must vanish. Figures 3 and 4 show that the boundary layer theory predicts adequately the degree of thermal stratification and the wall-to-wall temperature difference. In conclusion, the numerical solution verifies qualitatively and quantitatively the temperature field predicted by the boundary layer theory reported in the preceding section.

Figure 5 tests the main characteristic of the theoretical flow field, namely, the 'no-flow' condition which must prevail in the core. The figure shows the streamfunction in the vertical mid-plane of the porous layer. The remarkably flat central portion of the profile

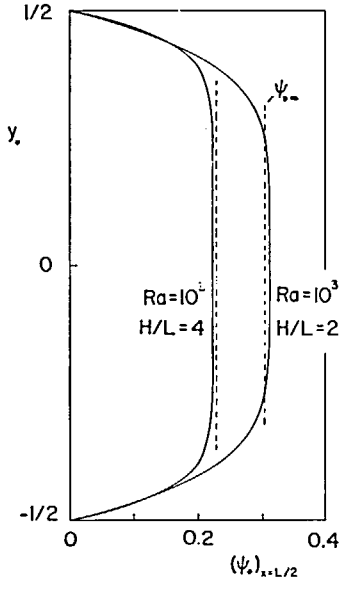

FIG. 5. Numerical results for the streamfunction in the vertical mid-plane $x = L/2$, and comparison with the theoretical core value $\psi_{*\infty}$.

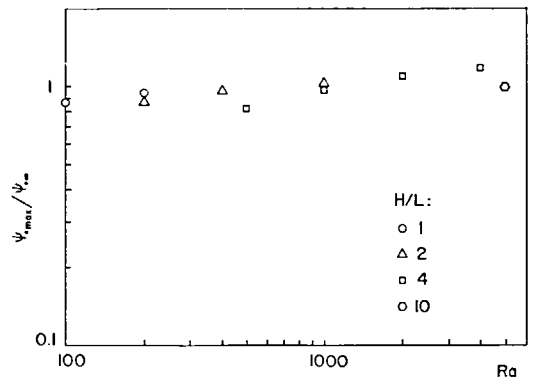

FIG. 6. The maximum numerical streamfunction value (ψ_{*max}) vs the theoretical core value ($\psi_{*\infty}$), for the ten cases (H/L, Ra) investigated numerically.

indicates that the fluid circulates only through relatively thin layers along the top and bottom walls, leaving the core region practically motionless. Thus, the core region between walls with uniform heat flux differs fundamentally from the core between isothermal walls: in the latter, core fluid motion is present at any level y_*, regardless of Rayleigh number [11].

Figure 5 shows also that the theoretical core streamfunction $\psi_{*\infty}$ agrees quantitatively very well with the numerical value of ψ_{*max}. Similar agreement was found in the remaining cases (H/L, Ra) solved numerically and listed in Table 1. Figure 6 shows the ratio $\psi_{*max}/\psi_{*\infty}$ in the range $100 < Ra < 5000$ covered by numerical simulations. In all cases, the match between theory and numerical experiment is within 17%. The fact that despite the width of the Ra range on Fig. 6, the ratio $\Psi_{*max}/\psi_{*\infty}$ does not vary appreciably is a strong indication that the boundary layer solution is correct.

Further evidence that the boundary layer solution is correct has been assembled in Fig. 7. The numerical solution discussed earlier in Figs. 3 and 4 showed that the most pronounced departure from the theoretical temperature pattern takes place in the vicinity of the top and bottom walls. Figure 7 shows this maximum departure in relative terms, as the ratio

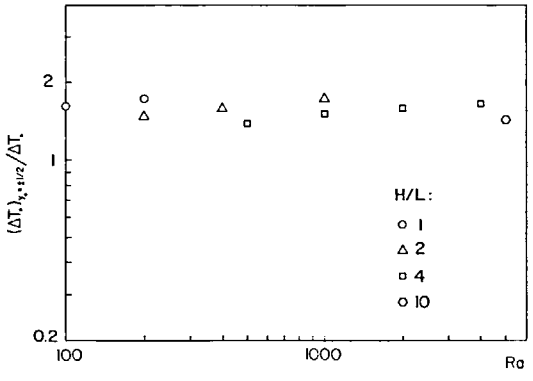

FIG. 7. The wall-to-wall temperature difference at $y = \pm H/2$, vs the theoretical value ΔT_* given by equation (32).

$(\Delta T_*)_{y_*=\pm 1/2}/\Delta T_*$ where ΔT_* is the theoretical value yielded by equation (32). It is clear that in the entire range $100 < Ra < 5000$ this ratio is practically constant (roughly 1.5). Therefore $(\Delta T_*)_{y_*=\pm 1/2}$ scales with the theoretical ΔT_*, in other words, the real temperature difference at *any* level along the vertical walls scales with the temperature difference derived theoretically for the boundary layer regime [equations (14) and (32)].

5. CONCLUDING REMARKS

This paper outlined an analytical solution for the phenomenon of heat and fluid flow by natural convection in a 2-dim. porous layer with uniform heat flux from the side. The analytical study focused on the boundary layer regime ($\delta \ll L$). The heat and fluid flow pattern was shown to differ substantially from the boundary layer regime in a layer with isothermal walls [8]. The main characteristics of boundary layer convection in a layer with uniform heat flux are:

(1) constant boundary layer thickness, of the order of $\delta/\lambda \sim H\,Ra^{-2/5}\,(H/L)^{-1/5}$;

(2) motionless core region ($u \to 0$, $v \to 0$);

(3) linearly stratified core region, with a vertical temperature gradient equal to

$$(\partial T/\partial y)_{\text{core}} = \left(\frac{q''}{k}\,Ra^{-1/3}\right)\lambda^2 = \frac{q''}{k}\,Ra^{-1/5}\left(\frac{H}{L}\right)^{2/5};$$

(4) wall temperature increasing linearly with altitude at the same rate as $(\partial T/\partial y)_{\text{core}}$, hence, altitude-independent temperature differences between walls;

(5) in any horizontal cut through the layer, an exact balance between the net upflow of enthalpy and the net downflow of heat conduction.

The main features of the theoretical boundary layer regime were tested and proven correct based on a complete numerical simulation of the phenomenon, in the range $100 < Ra < 5000$, $1 \leqslant H/L \leqslant 10$. As expected, the boundary layer solution breaks down in the vicinity of the top and bottom adiabatic walls. The height of the top and bottom end regions, δ_H, in which the theoretical boundary layer solution breaks down can be determined using scale analysis. The boundary layer stream $\rho v\delta$ enters the δ_H region and travels parallel to the adiabatic wall; from one end of the adiabatic wall to the next, the stream experiences an enthalpy drop of order $(\rho v\delta)c_p\Delta T$ caused by direct heat conduction to the core across a temperature difference of order ΔT and a conduction thickness δ_H. We have

$$\rho v\delta c_p \Delta T \sim kL\frac{\Delta T}{\delta_H}$$

or, using equations (9),

$$\frac{\delta_H}{H} \sim \frac{L}{H}\,Ra^{-1/3}.$$

Therefore, as H/L and Ra increase, the top and bottom regions δ_H decrease, and the vertical boundary layer regime occupies most of the porous layer. This trend is confirmed by Figs. 3 and 4 (both of which are for $Ra = 1000$): as H/L increases from 2 to 4, the top and bottom regions diminish in height. The same trend is confirmed by Fig. 5.

REFERENCES

1. K. J. Schneider, Investigation of the influence of free thermal convection on heat transfer through granular material, *Proc. Int. Inst. Refrig.* **11**, 247–253 (1963).
2. G. Mordchelles-Regnier, P. Micheau, A. Pirovano, C. Jumentier, J. S. Terpstra, Y. Lecourt, P. Cave and M. Breuille, *Recherches Recentes Effectuees en France sur l'Isolation Thermique des Reacteures Nucleaires*, pp. 529–544. International Atomic Energy Agency, Vienna (1969).
3. S. Klarsfeld, Champs de temperature associes aux mouvements de convection naturelle dans un milieu poreux limite, *Rev. Gen. Therm.* **108**, 1403–1423 (1970).
4. B. K. C. Chan, C. M. Ivey and J. M. Barry, Natural convection in enclosed porous media with rectangular boundaries, *Trans. Am. Soc. Mech. Engrs*, Series C, *J. Heat Transfer* **92**, 21–27 (1970).
5. C. G. Bankvall, Natural convection in vertical permeable space, *Wärme- und Stoffübertragung* **7**, 22–30 (1974).
6. P. J. Burns, L. C. Chow and C. L. Tien, Convection in a vertical slot filled with porous insulation, *Int. J. Heat Mass Transfer* **20**, 919–926 (1977).
7. C. E. Hickox and D. K. Gartling, A numerical study of natural convection in a horizontal porous layer subjected to an end-to-end temperature difference, *Trans. Am. Soc. Mech. Engrs*, Series C, *J. Heat Transfer* **103**, 797–802 (1981).
8. J. W. Weber, The boundary layer regime for convection in a vertical porous layer, *Int. J. Heat Mass Transfer* **18**, 569–573 (1975).
9. A. Bejan, On the boundary layer regime in a vertical enclosure filled with a porous medium, *Lett. Heat Mass Transfer* **6**, 93–102 (1979).
10. P. G. Simpkins and P. A. Blythe, Convection in a porous layer, *Int. J. Heat Mass Transfer* **23**, 881–887 (1980).
11. P. A. Blythe and P. G. Simpkins, Convection in a porous layer for a temperature dependent viscosity, *Int. J. Heat Mass Transfer* **24**, 497–506 (1981).
12. K. L. Walker and G. M. Homsy, Convection in a porous cavity, *J. Fluid Mech.* **87**, 449–474 (1978).
13. A. Bejan and C. L. Tien, Natural convection in a horizontal porous medium subjected to an end-to-end temperature difference, *Trans. Am. Soc. Mech. Engrs*, Series C, *J. Heat Transfer* **100**, 191–198 (1978).
14. A. Bejan and R. Anderson, Heat transfer across a vertical impermeable partition imbedded in porous medium, *Int. J. Heat Mass Transfer* **24**, 1237–1245 (1981).
15. E. M. Sparrow and J. L. Gregg, Laminar free convection from a vertical plate with uniform surface heat flux, *Trans. Am. Soc. Mech. Engrs* **78**, 435–440 (1956).
16. P. Cheng and W. J. Minkowycz, Free convection about a vertical plate imbedded in a porous medium with application to heat transfer from a dike, *J. Geophys. Res.* **83**, 2040–2044 (1977).
17. R. F. Bergholz, Natural convection of heat generating fluid in a closed cavity, *Trans. Am. Soc. Mech. Engrs*, Series C, *J. Heat Transfer* **102**, 242–247 (1980).
18. A. Bejan, Natural convection in a vertical cylindrical well filled with porous medium, *Int. J. Heat Mass Transfer* **23**, 726–729 (1980).
19. A. E. Gill, The boundary layer regime for convection in a rectangular cavity, *J. Fluid Mech.* **26**, 515–536 (1966).
20. A. Bejan, Natural convection heat transfer in a porous layer with internal flow obstructions, *Int. J. Heat Mass Transfer* **26**, 815–822 (1983).

REGIME DE COUCHE LIMITE DANS UNE COUCHE POREUSE AVEC UN FLUX DE CHALEUR UNIFORME LATERAL

Résumé—On donne une solution analytique et numérique de la convection naturelle dans une couche poreuse rectangulaire chauffée et refroidie avec des flux uniformes le long des parois verticales. On montre analytiquement que, dans le régime de couche limite, l'épaisseur de la couche limite verticale est constante (indépendante de l'altitude) et que la région centrale est sans mouvement. Le gradient de température vertical est le même et constant partout dans la couche poreuse. Des résultats numériques sont fournis pour $100 < Ra < 5000$, $1 \leqslant H/L \leqslant 10$, où $Ra = Kg\beta H^2 q''/(\alpha\nu k)$. La solution analytique de couche limite s'accorde bien avec les résultats numériques.

GRENZSCHICHTSTRÖMUNG IN EINER PORÖSEN SCHICHT MIT GLEICHFÖRMIGEN WÄRMESTROM VON DER SEITE

Zusammenfassung—In dieser Arbeit wird über analytische Lösungen und numerische Untersuchungen zur freien Konvektion in einer rechteckigen porösen Schicht, welche an den vertikalen Seitenwänden mit einem gleichförmigen Wärmestrom beheizt und gekühlt wird, berichtet. Die analytische Betrachtung zeigt, daß in der Grenzschichtströmung die Dicke der vertikalen Grenzschicht konstant ist (unabhängig von der Höhe) und im Kerngebiet keine Bewegung stattfindet. Der vertikale Temperaturgradient in der porösen Schicht ist konstant und überall gleich. Die numerischen Ergebnisse sind für die Bereiche von $100 < Ra < 5000$ und $1 \leqslant H/L \leqslant 10$, mit $Ra = Kg\beta H^2 q''/(\alpha\nu k)$, dargestellt. Die analytische Lösung für die Grenzschicht zeigt gute Übereinstimmung mit den numerischen Ergebnissen.

РЕЖИМ ПОГРАНИЧНОГО СЛОЯ В ПОРИСТОМ СЛОЕ ПРИ РАВНОМЕРНОМ НАГРЕВЕ СБОКУ

Аннотация—Представлено аналитическое решение и численное исследование естественной конвекции в прямоугольном пористом слое при равномерном нагреве и охлаждении его вертикальных боковых стенок. Аналитическое решение показывает, что в режиме пограничного слоя толщина вертикального пограничного слоя постоянна (не зависит от высоты), а область ядра неподвижна. Вертикальный температурный градиент также постоянен по всему пористому слою. Представлены численные результаты для диапазонов $100 < Ra < 5000$, $1 \leq H/L \leq 10$, где $Ra = Kg\beta H^2 q''/(\alpha\nu k)$. Показано, что аналитическое решение пограничного слоя хорошо согласуется с численными результатами.